HHS Public Access

Author manuscript

Nat Commun. Author manuscript; available in PMC 2015 October 13.

Published in final edited form as:

Nat Commun. ; 6: 6727. doi:10.1038/ncomms7727.

Plasticity of Hopx+ Type I alveolar cells to regenerate Type II cells in the lung

Rajan Jain[1,*], **Christina E. Barkauskas**[2,*], **Norifumi Takeda**[1,3], **Emily J. Bowie**[4], **Haig Aghajanian**[1], **Qiaohong Wang**[1], **Arun Padmanabhan**[1,5], **Lauren J. Manderfield**[1], **Mudit Gupta**[1], **Deqiang Li**[1], **Li Li**[2], **Chinmay M. Trivedi**[1,6], **Brigid L. M. Hogan**[4,#], and **Jonathan A. Epstein**[1,#]

[1]Department of Cell and Developmental Biology, Penn Cardiovascular Institute, Institute of Regenerative Medicine, Perelman School of Medicine at the University of Pennsylvania, Philadelphia, PA 19104, USA

[2]Division of Pulmonary, Allergy, and Critical Care Medicine, Department of Medicine, Duke Medicine, Durham, NC 27710, USA

[4]Department of Cell Biology, Duke Medicine, Durham, NC 27710, USA

Abstract

The plasticity of differentiated cells in adult tissues undergoing repair is an area of intense research. Pulmonary alveolar Type II cells produce surfactant and function as progenitors in the adult, demonstrating both self-renewal and differentiation into gas exchanging Type I cells. *In vivo*, Type I cells are thought to be terminally differentiated and their ability to give rise to alternate lineages has not been reported. Here, we show that *Hopx* becomes restricted to Type I cells during development. However, unexpectedly, lineage-labeled Hopx$^+$ cells both proliferate and generate Type II cells during adult alveolar regrowth following partial pneumonectomy. In clonal 3D culture, single Hopx$^+$ Type I cells generate organoids composed of Type I and Type II cells, a process modulated by TGFβ signaling. These findings demonstrate unanticipated plasticity

[#]Corresponding authors: Jonathan A. Epstein, Smilow Center for Translational Research, 09-105, 3400 Civic Center Blvd., Philadelphia, PA 19104, USA, Phone: 215-898-8731, Fax: 215-898-9871, epsteinj@upenn.edu. Brigid L.M Hogan, 388 Nanaline Duke Building, Box 3709, Duke Medicine, Durham, North Carolina 27710, USA, Phone: 919.684.8085, Fax: 919.684.8592, brigid.hogan@dm.duke.edu.

[3]Department of Cardiovascular Medicine, The University of Tokyo Hospital, 7-3-1 Hongo, Bunkyo, Tokyo 113-8655, Japan

[5]Massachusetts General Hospital, 55 Fruit St, Boston, MA 02114

[6]University of Massachusetts Medical School, 368 Plantation Street, Worcester MA 01605

[*]These authors contributed equally to this work.

Author Contributions

R.J., C.E.B, B.L.M.H., and J.A.E. designed experiments, analyzed data, and wrote the paper. R.J. and C.E.B. performed experiments. N.T. performed and analyzed pneumonectomy experiments. E.J.B., Q.W, A.P., L.L. assisted with histology, genetic manipulation and mouse husbandry. H.A. performed confocal analyses of images. L.M., M.G., and D.L., helped with lineage tracing experiments. C.M.T. performed microarray analyses.

Supplementary Information is linked to the online version of the paper at www.nature.com/naturecommunications.

Competing financial interest statement

Authors declare no competing financial interests.

Accession codes:

Microarray data have been deposited in GEO under accession code GSE65755.

of Type I cells and a bi-directional lineage relationship between distinct differentiated alveolar epithelial cell types *in vivo* and in single cell culture.

In the adult lung millions of air-exchanging units, termed alveoli, facilitate the transfer of oxygen from inhaled air into the blood stream. Mature alveoli are composed of two major distinct epithelial cell types, Type I and Type II cells. Type I cells are thin, have a large surface area, and lie in close contact with capillaries to facilitate gas exchange; they express Podoplanin (Pdpn) and AGER (Advanced Glycosylation End Product-specific Receptor). Type II cells are cuboidal and are defined by the production and secretion of surfactant proteins, including Surfactant Protein C (Sftpc), stored in specialized lamellar bodies. Studies in the 1960s and 70s demonstrated that Type II cells proliferate in response to injury and suggested they gave rise to Type I cells[1, 2]. Recent genetic fate-mapping experiments extended these findings and showed that Type II cells function as progenitors in the adult lung during homeostatic conditions and upon Type II cell ablation[3, 4]. Lineage-labeled Type II cells both self-renew and generate Type I cells *in vivo* and in clonal 3D organoid cultures *ex vivo*[3, 4]. Elucidating the mechanisms by which alveolar cell types are maintained and regenerated after injury has important implications for normal respiratory physiology and disease, and for designing regenerative therapies. An important outstanding question, however, is whether Type I cells can change their phenotype and participate in regenerative responses *in vivo*.

An emerging paradigm in stem cell biology is that some tissues employ “facultative” progenitors that differentiate in one direction under physiologic conditions but may de-differentiate or transdifferentiate during repair following injury[5, 6, 7]. Multiple studies have highlighted this phenomenon in invertebrates[8], but few examples have been documented in mammals, especially involving post-mitotic differentiated cells[5]. Previous studies suggested that isolated Type I-like cells can be induced to express non-Type I cell markers *in vitro*[9, 10]. However, it remains an open question as to whether and under what conditions Type I cells exhibit a phenotypic switch *in vivo*. Here, we demonstrate that adult, differentiated Type I cells, marked by expression of the atypical homeodomain-containing protein Hopx, can, under repair conditions, both self-renew and give rise to Type II cells. Under the same conditions, the differentiation of Type II to Type I cells increases. These findings reveal a bi-directional lineage relationship between the differentiated cell types of the alveolar epithelium in response to physiological need.

Results

Hopx marks bipotent embryonic alveolar progenitors

Early lung development is characterized by branching morphogenesis that results in a bronchiolar tree[11, 12]. Lineage tracing studies have shown that early tip cells that express *Id2* and *Sox9* are multipotent, but evidence suggests that as development proceeds they become restricted in developmental potential and later give rise only to alveolar cell

types[4, 13, 14, 15, 16]. However, the identity and *in vivo* potential of individual late distal progenitor cells is still incompletely understood, requiring new lineage markers. Hopx is first expressed in the embryonic lung at embryonic day (E) 15.5, as judged by immunohistochemistry for both native protein and a "knock-in" reporter allele in which GFP and Flag are expressed in Hopx$^+$ cells[17]. Specifically, Hopx is robustly expressed in the stalk cells of terminal end buds and excluded from surrounding mesenchyme (Fig. 1a). Hopx is also detected in a subset of Sox9$^+$ cells near the distal tips (Fig. 1b). A subset of these distal Hopx$^+$ cells also co-express Sftpc, Pdpn, and AGER (Fig. 1a, c, d and Supplementary Fig. 1a, b). Our previous studies have implicated Hopx as an important regulator of lung development[18]. Gene ontology analysis of microarray data from whole *Hopx*$^{-/-}$ and *Hopx*$^{+/+}$ E16.5 lungs confirmed significant changes in the expression of genes categorized as relevant to regulation of lung development and glyco- and lipoprotein expression (Supplementary Dataset 1).

To determine the fate of embryonic *Hopx*$^+$ cells, we performed lineage-tracing experiments using *Hopx*$^{ERCre/+}$ mice and R26 reporter alleles[19]. To establish the validity of this approach, *Hopx*$^{ERCre/+}$*; R26*$^{Tomato/+}$ (*R26*$^{Tom/+}$) embryos were treated with a single dose of tamoxifen at E15.5 and lungs collected 24 hours later. Lineage labeling results in nuclear and cytoplasmic RFP/Tomato expression and analysis confirmed the presence of a few, scattered, single Tom$^+$ cells (Fig. 1e) specifically within the distal domain of Hopx expression (Supplementary Fig. 1c-f). Lungs were then analyzed at E18.5. Tom$^+$ cells co-express either Pdpn, (Fig. 1f) or Sftpc (Fig. 1g). At P0, we detected clusters of lineage-labeled cells that were composed of both Type I and Type II cells (Fig. 1h). Longer chases, up to 3 months postnatally, confirmed that Hopx-derived Type I and Type II cells are long lived (Supplementary Fig. 2a, b), and can be found in clusters, suggesting proliferation of Hopx-derived cells. (Fig. 1i, Supplementary Fig. 2c, d). Some of these clusters contained lineage-labeled Type I cells intermixed with Type II cells in discrete areas (Supplementary Fig. 2d). Taken together, the results from these lineage tracing experiments are consistent with recent single-cell RNA-seq studies suggesting that Hopx-expression marks a bipotent alveolar progenitor[4, 14].

Alveoli continue to mature postnatally (reviewed in [20]). When *Hopx*$^{ERCre/+}$*; R26*$^{Tom/+}$ mice were given a single dose of tamoxifen at P5 and analyzed at P28, both lineage-labeled Type I and II cells were identified (Supplementary Fig. 2e, f). However, labeling of Hopx cells at P35 and analysis at P46 revealed only lineage-labeled Pdpn$^+$ Type I cells (Supplementary Fig. 2g). No Tom$^+$ Sftpc$^+$ could be identified among thousands counted (Supplementary Fig. 2h; 0/2334 Sftpc$^+$ cells were Tom$^+$, n=3 mice). This suggests that during the first month of postnatal life Hopx$^+$ normally becomes restricted to cells with the phenotype of differentiated Type I cells (Fig. 1j).

Hopx$^+$ cells give rise to Type II cells during lung regrowth

Analysis of the adult lung confirms that Hopx, a transcription co-factor[21], is robustly expressed in the nuclei of cells that are Type I, Pdpn$^+$ and AGER$^+$ (Fig. 2a, b red arrowhead). However, no expression is detected in Sftpc$^+$ Type II cells (Fig. 2c, d, 0/2276 Sftpc$^+$ cells observed in 22 sections, n= 4 mice spanning P35-P133). We also failed to detect

Hopx expression in Sftpc$^+$, Scgb1a1$^+$ cells, also known as bronchiolar alveolar stem cells (BASCs)[22], at the bronchiolar alveolar duct junction (Fig. 2e, f). We performed short-term lineage tracing of Sftpc$^+$ cells by pulsing *Sftpc$^{ERCre/+}$; R26$^{Tom/+}$; Hopx$^{3XFlag/+}$* adult mice with tamoxifen every five days for 15 days (4 doses); mice were sacrificed 3 days later. We did not detect any Hopx-expressing (GFP$^+$) cells derived from adult Sftpc$^+$ cells (Tom$^+$) under homeostatic conditions (Fig. 2g, 0/1847 Tom$^+$ cells were GFP$^+$), consistent with our earlier report[3]. Finally, quantitative RT-PCR analysis of FACS sorted lineage-labeled Sftpc$^+$ and non-lineage labeled, Pdpn$^+$ alveolar cells from *Sftpc$^{ERCre/+}$; R26$^{Tom/+}$* adult mice is consistent with our conclusion that Hopx becomes restricted to Type I cells in the adult alveolus and is excluded from Type II, Sftpc$^+$ cells (Fig. 2h).

In adult mice, unilateral pneumonectomy results in compensatory growth and "realveolarization" of the remaining lung tissue[23], including the formation of new secondary septa over a period of approximately 2 weeks, but the source of new alveolar cells is not well defined (reviewed in[24]). To investigate whether Type I cells contribute to the regrowth and remodeling we gave a *Hopx$^{ERCre/+}$*; *R26$^{mt\text{-}mg/+}$* mouse a single dose of tamoxifen at P90 to lineage trace Hopx-expressing cells. Labeled cells expressed membrane-bound GFP. The left lung was then removed 19d after tamoxifen administration (Fig. 3a). As expected, GFP$^+$ lineage labeled Pdpn$^+$ Type I cells were present in the alveoli of the resected lung segment (Supplementary Fig. 3a), and we could not detect any labeled Sftpc$^+$ cells that might have been derived from Hopx-expressing precursors (Supplementary Fig. 3b). The mouse was sacrificed 7 days later and the remaining right-sided lobes were analyzed. This revealed an increase in number of Hopx-derived, GFP$^+$ cells after pneumonectomy (Fig. 3b-d), many of which express Pdpn (Supplementary Fig. 3c). Consistent with this observation, there was an increase in the percentage of Hopx$^+$ that were phospho-histone H3$^+$ at day 3 and 7 after pneumonectomy compared to sham, wildtype control mice (Supplementary Table 1). At 7d we also unexpectedly found rare Hopx-derived cells that express the Type II marker Sftpc (Fig. 3e-g). We then repeated these experiments in *Hopx$^{ERCre/+}$*; *R26$^{Tom/+}$* mice using a single pulse of low dose tamoxifen at P102 (50 mg/kg instead of 100 mg/kg, followed by a washout period averaging 20 days (range: 17-21 days, n=3) prior to pneumonectomy, Fig. 3a). In these experiments, we analyzed the remaining lungs 21 days after pneumonectomy and observed Hopx-derived Sftpc$^+$ cells that had persisted for at least this time (Fig. 3h, i and Supplementary Fig. 4a-c). Analysis revealed 18 Sftpc$^+$, Hopx-derived cells out of a total of 656 Sftpc$^+$ cells counted (~1 Sftpc$^+$-lineage labeled cell per 700 μm^2 high-powered field in 16 sections, n=3 animals) compared with pre-pneumonectomy control samples in which 0/1156 Sftpc$^+$ cells were lineage-labeled (n=3 animals, at least 3 sections quantified from each, ($p<0.001$, two-tailed t-test) Supplementary Fig. 4d). These data indicate that by 21 days post-pneumonectomy approximately 2.7% of Type II cells are derived from Hopx$^+$ cells. However the *Hopx$^{ERCre/+}$* allele is relatively inefficient, with only 29 ± 1.5% of Hopx$^+$ nuclei being lineage labeled at the time of pneumonectomy (average ± S.D., Supplementary Fig. 4e). This suggests that the contribution of Type 1 to Type II cells is in fact 9.4%. These experiments also confirmed an expansion of Hopx-derived alveolar cells (2.1 fold increase in percentage of Tom$^+$ nuclei post-pneumonectomy versus pre-pneumonectomy, $p=0.045$, paired two-tail t-test, Supplementary Fig. 4f, g), suggesting that Hopx$^+$ cells are capable of self-renewal.

We performed two important control experiments to support the validity of our findings. First, sham-operated animals, in which the left lung was not removed, did not show any lineage labeled Sftpc$^+$ cells 21 days after the operation (Supplementary Fig. 5a-d, 0/1686 Sftpc$^+$ cells counted were Tom$^+$, n=3 animals). Second, pneumonectomy of a *Hopx$^{3XFlag/+}$* mouse at P102 did not result in any Hopx$^+$, Sftpc$^+$ cells at 7 days (0/393 and 0/449 Sftpc$^+$ cells were Hopx$^+$ in sham operated animals and post-pneumonectomy animals, respectively; Supplementary Fig. 5e-f). This control shows that Hopx expression is not activated in Sftpc$^+$ Type II cells in response to the regrowth stimulus.

In parallel experiments, we performed pneumonectomies on *Sftpc$^{ERCre/+}$*; *R26$^{Tom/+}$* mice after treatment with tamoxifen to determine if lineage-labeled Type II cells give rise to Type I cells during adult lung regrowth. Prior to pneumonectomy and in sham control animals, only DC-LAMP$^+$ cells in the alveoli were lineage-labeled cells ([3] and Fig. 4a), with little differentiation into Type I cells, as previously described. DC-LAMP is a glycoprotein found in lamellar bodies in mature Type II cells. By contrast, 21 days post-pneumonectomy, many lineage-labeled Hopx$^+$ Type I cells were readily identifiable, particularly in the periphery of the lung (Fig. 4b-d; 16.0 ± 5.2% RFP$^+$ cells were Hopx$^+$, n=3 animals) where remodeling has been shown to be highest[24]. Taken together, our data show that during compensatory regrowth of the adult lung both Sftpc$^+$ Type II and Hopx$^+$ Type I cells contribute to the formation of new alveoli and undergo both proliferation and bi-directional differentiation.

Single Type I cells form organoids *ex vivo*

We sought to confirm our evidence for Type I cell transdifferentiation using methods independent of *Hopx$^{ERCre/+}$* lineage tracing, and to further define the plasticity of individual Hopx$^+$ Type I cells. We therefore adapted a 3D culture system for Type II cells[3] to test the developmental potential of Type 1 cells. In the original assay individual Type II cells both self renew and give rise to Type I cells, forming 3D organoids. We hypothesized that individual Hopx$^+$ Type I cells dissociated from these organoids would generate Type II cell-containing organoids in clonal culture conditions. To test our hypothesis, adult *Sftpc$^{ERCre/+}$; Hopx$^{3XFlag/+}$; R26$^{Tom/+}$* mice were treated with tamoxifen and 1-2 days after the final dose a single cell suspension was prepared. Tom$^+$ (lineage labeled Type II) cells were isolated by FACS and plated at clonal density with *PDGFR*α+ stromal cells isolated from a separate cohort of mice (Fig. 5a). By day 16 of culture, organoids containing lineage-labeled Sftpc$^+$ Type II cells and lineage-labeled (RFP$^+$) Type I cells were present; the Type I cells expressed GFP from the *Hopx$^{3XFlag/+}$* allele (Fig. 5b). Spheres were then dissociated and lineage-labeled Type II and Type I cells were isolated, separated by FACS and replated individually in organoid culture. Within 14 days, both Type I and Type II cells gave rise to spheres (Fig. 5c-h). As previously described[3], spheres derived from Type II cells generated both Type I and Type II cells (Fig. 5c-e). Importantly, spheres derived from isolated Type I cells were also composed of both Type I and Type II cells (Fig. 5f-h). We then dissociated Type I derived organoids (Fig 5f-h), separated Type I and II cells based on differential endogenous Pdpn expression, and grew them again in organoid culture. Both cohorts of cells were able to generate organoids containing Type I and II cells, demonstrating that Type I cells can give rise to Sftpc$^+$, Type II cells that retained the ability to self renew and

differentiate (Supplementary Fig. 6a). Therefore, we conclude that differentiated Type I and II cells can interconvert.

We then confirmed that plasticity is a property of freshly isolated Type I cells using two complementary approaches. *Hopx*$^{ERCre/+}$*; R26*$^{Tom/+}$ mice were injected with tamoxifen to label Type I cells, and three days later, Type I cells were isolated by FACS (Tom$^+$ EpCAM$^+$ Pdpn$^+$; Fig. 5i). Isolated cells were placed in clonal organoid culture, and by day 14, lineage-labeled Type I and II cells were present (Fig. 5j-m). In a parallel approach, we cultured Type I cells and lineage-labeled Type II cells isolated by FACS from *Sftpc*$^{ERCre/+}$*; Hopx*$^{3XFlag/+}$*; R26*$^{Tom/+}$ mice (Tom$^-$ EpCAM$^+$ Pdpn$^+$ GFP$^+$ and Tom$^+$ EpCAM$^+$ Pdpn$^-$ GFP$^-$ cells, respectively, Fig. 5n, Supplementary Fig. 6b). Quantitative RT-PCR confirmed that *Hopx* and *Sftpc* were significantly enriched in the isolated Type I and Type II populations, respectively (Supplementary Fig. 6c). The Type I cell-derived-organoids were composed of Hopx/GFP$^+$ Pdpn$^+$ Type I cells and Sftpc$^+$ Type II cells (Fig. 5o-q). Taken together, the above experiments demonstrate that single Hopx$^+$, Type I cells possess the capacity to give rise to organoids composed of Pdpn$^+$, Type I cells and Sftpc$^+$, Type II cells *ex vivo*.

In order to gain insight into the mechanism of Type I cell to Type II conversion, we repeated the organoid culture experiments as in Fig. 5a-h. We hypothesized that pathways known to be important regulators of lung development and homeostasis[24, 25, 26, 27, 28] also regulate the interconversion of Type I and Type II cells and we used our organoid system to test the importance of candidate signaling pathways in this process. Specifically, organoids were prepared using lineage-labeled Type II cells from *Sftpc*$^{ERCre/+}$*; Hopx*$^{3XFlag/+}$*; R26*$^{Tom/+}$ mice. After 15 days in culture, organoids were dissociated into a single cell suspension and lineage-labeled Type II and Type I cells were isolated, and separated by FACS. Triplicate samples of 3000 cells of each phenotype were then replated at clonal density with Pdgfra$^+$ fibroblasts in the presence of small molecules and agonists/antagonists of TGFβ, Wnt and Notch signaling pathways or vehicle control (Fig. 6; Supplementary Figs. 7-8).

At 14 days of culture, we noted that treatment with 5μM LY2157299 resulted in a significant increase in the colony forming efficiency (CFE) of organoids derived from Type I cells (Fig. 6a-d). CFE of organoids from Type II cells was not significantly affected (Fig. 6e-h), but for both cell types the size of spheres was increased to about the same extent (Fig. 6 and Supplementary Fig. 7). LY2157299 is a TGFβ receptor I kinase inhibitor that potently blocks the TGFβ signaling pathway by inhibiting the de-novo phosphorylation of pSmad2[29]. Consistent with a direct effect of the inhibitor on TGFβ signaling in epithelial cells we identified Hopx$^+$ pSmad2/3$^+$ cells in control spheres and a reduction in LY2157299-treated cultures (Fig. 6c, g). These data suggest that inhibition of TGFβ signaling preferentially augments the ability of a single Type I cell to give rise an organoid containing both Type I and Type II cells. Though pSmad2/3 was robustly expressed in Hopx$^+$, Type I cells in control cultures (Fig. 6c, g), we cannot rule out a non-cell autonomous effect of TGFβ inhibition in our culture system. Treatment of both Type I and Type II cultures resulted in larger organoids (Supplementary Fig. 7). Treatment with recombinant TGFβ1 did not significantly affect CFE (Supplementary Fig. 8a, b, f), perhaps because the pathway is already stimulated under our organoid culture conditions. Modulation of the Wnt and Notch signaling pathways failed to augment Type 1 to Type II conversion (Supplementary Fig. 8).

Discussion

Emerging reports suggest that adult stem and progenitor cell populations exploit a variety of mechanisms to maintain tissue homeostasis[5, 8, 30, 31]. Previously, we demonstrated that the crypt of the mouse small intestine harbors two anatomically distinct populations of intestinal stem cells that are in dynamic equilibrium in steady state[19]. Our current findings with the adult lung suggest that interconversion can take place among differentiated cell types to maintain tissue integrity in the setting of repair *in vivo*. Prior work by our group and others has demonstrated that adult Type II alveolar cells can generate Type I cells under homeostasis and partial Type II cell ablation[3, 4]. Our present studies establish that the reverse is also true *in vivo* and that a bidirectional lineage relationship exists between Type I and Type II cells during lung regrowth. Available tools and reagents do not allow us to determine if conversion of Type I cells to Type II cells during regeneration necessitates "dedifferentiation" to an embryonic-like bipotent state, or whether the conversion is "direct". Regardless, it is clear that neither Type I nor Type II cells are "terminally" differentiated and both retain unexpected plasticity into adulthood. These findings have important implications for regenerative medicine and for cancer. Indeed, interconversion of differentiated cell types makes discussion of the "cell of origin" of certain cancers complex. Type II cells can be a cell of origin for lung adenocarcinoma based upon the analysis of tumors produced by activation of Kras in Type II cells[4, 32, 33]. However, we found that Kras activation in $Hopx^{+}$ cells also produces tumors. Some tumors arising from $Hopx^{+}$ cells expressed Sftpc, suggesting that lineage plasticity may be hijacked during carcinogenesis (Fig. 7). Ongoing studies focused on cellular reprogramming and transdifferentiation coupled with increasingly sophisticated clonal analysis techniques may reveal unexpected plasticity in adult organs and tissues that contribute to homeostasis, tissue repair and to disease.

Methods

$Hopx^{ERCre/+}$, *$Hopx^{3XFlag/+}$*, *$Sftpc^{ERCre/+}$*, *K-$Ras^{G12D/+}$*, *$R26^{mT\text{-}mG/+}$*, *$R26^{Tom/+}$*, *$Hopx^{LacZ/+}$*, and B6.129S4-*$Pdgfra^{tm11(EGFP)Sor}$*/J (*Pdgfra-H2B:GFP* - from the Jackson Laboratory) mice have been described previously [3, 17, 19, 21, 33, 34, 35]. Hopx expression in the *$Hopx^{3XFlag/+}$* allele can be detected by GFP or Flag expression, as a *3XFlag-viral-2A-GFP* sequence was engineered into the 3' UTR of the *Hopx* locus to append the final coding exon. Our previous studies demonstrate that GFP and Flag expression faithfully recapitulate Hopx expression[17]. A second, different *$R26^{Tom/+}$* mouse allele[36] was used specifically in crosses performed that included *$Sftpc^{ERCre/+}$*. All mice were maintained on mixed genetic backgrounds. The University of Pennsylvania and Duke University Institutional Animal Care and Use Committee approved all animal protocols.

Lineage tracing experiments

Mice were injected intraperitoneally or gavaged with 100mg/kg body weight tamoxifen (Sigma) dissolved in corn oil unless otherwise indicated, as either a single or multiple doses, as indicated. For experiments represented in Fig. 2h, mice were injected every other day with 200 mg/kg body weight tamoxifen starting at P188 for a total of 4 doses; mice were

sacrificed at P196. For experiments represented in Fig. 4n, mice were dosed with 200 mg/kg body weight tamoxifen for a total of 4 doses. Age of mice at time of tamoxifen injection is as indicated in the text and figures.

Pneumonectomy

Mice were anesthetized with a mixture of ketamine (100 mg/kg), xylazine (2.5 mg/kg) and acepromazine (2.5 mg/kg). Mice were then placed in the supine position, an endotracheal tube was inserted, and mice were ventilated using a volume-cycled rodent ventilator (MiniVent Type 845; tidal volume of 0.4 ml room air, respiratory rate of 110 breaths/minute). The thoracic cavity was exposed by incising the fifth left intercostal space. The left lung was gently lifted through the incision, and then a 5-0 silk suture was tied around the hilum. The hilum was transected distal to the tie using forceps and microdissecting scissors (n=4 mice total). Sham-operated mice (n=4 total) underwent the identical surgical procedure, including isolating the left hilum, but without the resection of left lung. $Hopx^{ERCre/+}$; $R26^{mT\text{-}mG/+}$ mice were pulsed with a single dose of tamoxifen (intraperitoneal, 100 mg/kg) at P90 and pneumonectomy (or sham, n=1 for each condition) was performed at P109. The mice was sacrificed 7 days after the surgery. $Hopx^{ERCre/+}$; $R26^{Tom/+}$ mice were pulsed with a single dose of tamoxifen (intraperitoneal, 50 mg/kg) at P102, and pneumonectomy (or sham, n=3 for each pneumonectomy and sham) was performed at P118-121 (average washout period 20 days, range: 17-21 days) and mice were sacrificed 21 days later. Lungs were visualized on a Olympus MVX10 fluorescent dissecting microscope. Sftpc-lineage labeled mice (related to Fig. 4; 11 weeks of age at time of tamoxifen administration; 16 weeks of age at sacrifice) and C57/Bl6 mice (related to Supplementary Table 1; 10 weeks of age at sacrifice) underwent sham or pneumonectomy as indicated in a similar fashion as that outlined above. All pneumonectomy experiments were performed with male mice (70-121 days old). Nuclei were identified based on DAPI-positivity or based on cellular morphology. Quantification was performed manually and using ImageJ software.

Lung dissociation and FACS

Lung dissociation and cell sorting was done as described previously[3]. In brief, lungs were inflated with a protease solution [2-3mL per mouse; Collagenase Type I (450 U/mL; Gibco), Elastase (4U/mL; Worthington Biochemical Corporation), Dispase (5U/mL; BD Biosciences), and DNaseI (0.33 U/mL) in DMEM/F12][36], cut into small pieces, and then incubated at 37°C with frequent agitation. The resulting suspension was filtered, washed, incubated at room temperature in red blood cell lysis buffer (eBioscience), washed again, and resuspended in DMEM + 2% BSA. When antibody staining was required, lung suspension was blocked in 1% FcX TruStain (#101320; Biolegend) in 2% FBS, 2% BSA in 1x PBS. Antibodies used were: rat, EpCAM-BV711 (1:800, #563134; BD Horizon); hamster, Podoplanin-PE/Cy7 (1:250, #127412; Biolegend). Sorting was performed on FACS Vantage SE, and data were analyzed with FACS Diva (BD Biosciences).

For experiments related to Fig. 2h, a single cell suspension from the lungs of $Sftpc^{ERCre/+}$; $R26^{Tom/+}$ was made and first cells $Tomato^{+}$ were isolated via FACS (Tom^{+} being lineage

labeled Type II cells and their immediate derivatives). Tom$^-$ cells were then sorted based upon Pdpn expression to isolate Type I cells (Tom$^-$, Pdpn$^+$). For experiments related to Fig. 5a-h, cells Tom$^+$ cells were first isolated via FACS and then grown in organoid culture (Fig. 5b). Organoids from 5b were dissociated, Tom$^+$ cells were isolated via FACS based on Pdpn expression (Tom$^+$, Pdpn$^+$ = Type I cells, Tom$^+$, Pdpn$^-$ = Type II cells) and then grown in organoid culture. For experiments related to Fig. 5i-m, Tom+, EpCAM$^+$, Pdpn$^+$ cells were defined as Type I cells and plated in organoid culture. For experiments related to Fig. 5n-q, Tom$^-$ cells were first isolated via FACS and then subsequently sorted based on Hopx/GFP and Pdpn expression. Tom$^-$, Hopx$^+$, Pdpn$^+$ cells were plated in culture (Hopx$^+$, Type I cells).

Organoid culture

Stromal cells were obtained via FACS from *Pdgfrα-H2B:GFP* mice based upon GFP expression. As the GFP expressed by the Pdgfrα+ stromal cells express is purely nuclear, it has an appearance unlike the GFP driven by Hopx expression in *Hopx$^{3xFlag/+}$* mice, which is nuclear and cytoplasmic. Epithelial cells were sorted based upon lineage label and/or cell surface marker expression to discern Type II and Type I cells from all others. FACS-sorted cells were resuspended in MTEC/Plus and mixed 1:1 with growth factor-reduced Matrigel (BD Biosciences)[3]. 5×10^3 epithelial cells (unless otherwise indicated) and 5×10^5 stromal cells were seeded in 90 μl MTEC/Plus:Matrigel in individual 24-well 0.4-μm Transwell inserts (Falcon). CFE and histology were assessed between days 14 and 16. For passaging experiments, spheres were dissociated from Matrigel with the addition of 60μL Dispase to the insert and subsequent incubation at 37°C for 30 minutes. *Pdgfrα-H2B:GFP* mice were wildtype at the *Hopx* and *Sftpc* loci. For experiments related to Fig. 5a-h, *Sftpc$^{ERCre/+}$; Hopx$^{3XFlag/+}$; R26$^{Tom/+}$* mice, age 129 days or older, were pulsed 4 times with tamoxifen and sacrificed 1-2 days after the final dose. For experiments related to Fig. 5i-m, *Hopx$^{ERCre/+}$; R26$^{Tom/+}$* mice were injected every other day (between P96 and P102) with tamoxifen and three days later Type I cells were isolated by FACS. For experiments related to Fig. 5n-q, *Sftpc$^{ERCre/+}$; Hopx$^{3XFlag/+}$; R26$^{Tom/+}$* mice were at least P43 or older. For the screen of candidate signaling pathways, the following small molecules / recombinant proteins were used: LY2157299 (Selleck; 5μM); TGFβ1 (R&D; 0.2 ng/mL); DBZ (Millipore; 1 μM); CHIR99021 (Tocris; 3 μM); XAV939 (Tocris; 1 μM); or vehicle control.

Histology

Lungs were fixed in 2% paraformaldehyde, ethanol dehydrated, embedded in paraffin, and sectioned in the coronal plane, unless otherwise noted. Antibodies used were: GFP (goat, Abcam and rabbit, Molecular Probes, 1:100-1:200), RFP (recognizes tdTomato; rabbit, Rockland, 1:250 and mouse, Abcam, 1:50-1:250), Sftpc (rabbit, Millipore, 1:250-1:500), Pdpn (mouse, Developmental Studies Hybridoma Bank, 1:50-1:100), Sox9 (rabbit, Santa Cruz, 1:100), Sox2 (rabbit, Seven Hills Bioreagents, 1:1500 and goat, Santa Cruz, 1:500), Flag (mouse, Sigma, 1:100-1:250), Cdh1 (rabbit, Cell Signaling, 1:100), Hopx (rabbit, Santa Cruz, 1:100), AGER (rat, R&D, 1:50), phospho-histone H3 (mouse and rabbit, Cell Signaling, 1:20), DC-LAMP/CD208 (rat, Dendritics, 1:250), phospho-Smad 2/3 (rabbit, Cell Signaling, 1:250). For Sftpc and RFP double staining, sections were first incubated

1:250-1:500 anti-Sftpc for two days at 4°C. After washing, sections were incubated in 1:250 Alexa Fluo 488 AffiniPure Fab Fragment Goat anti-rabbit IgG (Jackson Immunoresearch) for two hours at room temperature. Subsequently, sections were co-stained with 1:50-1:250 anti-RFP and then the secondary antibody (1:250 Alexa Fluo 568 Goat anti-rabbit IgG or ImmPRESS Anti-Rabbit IgG). Further specific details of antibodies and immunhistochemistry are available upon request and basic staining protocols can be viewed at: http://www.pennmedicine.org/heart/research-clinical-trials/core-facilities/histology-gene-expression/. For 3D imaging of whole-mount lung lobes, tissue was cleared with Sca*l*eA2 reagent (4M urea, 0.1% wt/vol Triton X-100, 10% wt/wt glycerol in water[37]). After fixation in 4% PFA and washing in PBS, tissue was placed in Sca*l*eA2 and kept on a rocker for 1-2 weeks at 4°C until maximal tissue clearing occurred. Multiphoton images were acquired on an Olympus FV1000 with 25x/0.9 NA Sca*l*eView immersion lens. All immunohistochemistry was visualized on a Nikon Eclipse 80i fluorescence microscope, except the confocal images, which were evaluated on a Leica TCS SP8 or Zeiss 710 inverted confocal microscope. FIJI software was used to generate 3D volume rendering of a Z-stack images related to Fig. 3e (3D viewer plugin). All images were analyzed using Adobe Photoshop (version CS6), ImageJ (version 1.0), and/or FIJI (version 1.49b) (sizing, brightness or contrast adjustments, etc). Brightness and contrast were adjusted linearly across the entire image for any particular image, including individual color channels for merged images.

Quantitative Real-time-PCR

Gene expression levels were quantified by qRT-PCR on the StepOne Plus Real-Time PCR System (Applied Biosystems). RNA was isolated using a RNAqueous-Micro Kit (Ambion) from three biological replicates for each experimental group. cDNA was synthesized using an iScript cDNA Synthesis Kit (Bio-Rad) (34.5 ng RNA used as template for experiment reported in Fig 2H; 30 ng RNA used as template for experiment reported in Supplementary Fig. 6c.) Samples were run in triplicate, and 18 µl reactions were pipetted from a master mix with 2µl sample cDNA, 20µl 2x iQ SYBR Green Supermix, 10µl water, and 8µl primers (200 nM each). Threshold cycle values (Ct) for triplicate samples were averaged and normalized to Gapdh (ΔCt), and these values across samples were compared (ΔΔCt) to quantify relative expression. Primers are as follows: Gapdh: Forward 5'-AGG TCG GTG TGA ACG GAT TTG-3', Reverse 5'-TGT AGA CCA TGT AGT TGA GGT CA-3'; Sftpc: Forward 5'-CAA ACG CCT TCT CAT CGT GGT TGT-3', Reverse 5'-TTT CTG AGT TTC CGG TGC TCC GAT-3'; Pdpn: Forward 5'-ACC GTG CCA GTG TTG TTC TG-3', Reverse 5'-AGC ACC TGT GGT TGT TAT TTT GT-3'; Hopx: Forward 5'-TTC AAC AAG GTC AAC AAG CAC CCG-3', Reverse 5'-CCA GGC GCT GCT TAA ACC ATT TCT-3'. Data are reported as relative quantification (RQ); error bars represent 95% confidence intervals.

Microarray Analysis

Microarray analysis was performed using three independent samples of $Hopx^{+/+}$ and $Hopx^{LacZ/LacZ}$ (null) lung tissue from E16.5 embryos. RNA was extracted and reverse transcribed without amplification. Microarray analysis was performed by the University of

Pennsylvania Microarray Core Facility using Affymetrix mouse cDNA arrays (Affymetrix Mouse Genome Arrays 430 v2.0). Cel files were RMA normalized using Partek Genomics Suite v6.6, and SAM (Significant Analysis of Microarray) was used to analyze the data. Rma-normalized log2-transformed intensities are reported. The supplementary dataset includes information for genes with greater than 1.2 fold or less than -1.2 fold change in *Hopx*$^{-/-}$ tissues compared to control. Gene ontology analysis was performed with the top 1500 genes that were upregulated based on fold change (since Hopx is known to be a repressor). Analysis was performed by inputting those Affymetrix Probe ID numbers into: http://david.abcc.ncifcrf.gov. Microarray data have been deposited in GEO under accession code GSE65755.

Statistical Analysis

Two-tailed t-test was used to analyze the percentage of lineage-labeled Sftpc^{+} cells in each mouse from pneumonectomy experiments. Eighteen lineage-labeled Sfptc^{+} cells were identified from 16 sections from 3 post-pneumonectomy animals. At least four sections were quantified from each animal. Paired two-tailed t-test was used to compare the percentage of RFP^{+} cells pre- and 21 days post-pneumonectomy. Three pre-pneumonectomy and 3 post-pneumonectomy replicates were compared, and at least 3 sections were quantified from each replicate. Two-tailed t-test was used to analyze the colony forming efficiency and average sphere diameter of organoids. Two-tailed t-test was used to analyze the percentage of phospho-histone H3^{+} cells.

Supplementary Material

Refer to Web version on PubMed Central for supplementary material.

Acknowledgments

We thank the Epstein and Hogan laboratories for helpful discussions. We thank Lili Guo for help with figures. We thank Ed Morrisey for critical reading of the manuscript and helpful discussions. We thank Andrea Stout and Penn CDB imaging core for help with imaging. We thank John Tobias for help with microarray analyses. This work was supported in part by funds from the NIH to J.A.E (U01HL110942, RO1HL071546), R.J. (K08HL119553-02), C.E.B. (K08HL122521-01) and B.L.M.H (UO1HL111018). Work was also supported by grants within the NIH Lung Repair and Regeneration Consortium (UO1HL110967), and by the Cotswold Foundation.

References

1. Evans MJ, Cabral LJ, Stephens RJ, Freeman G. Transformation of alveolar type 2 cells to type 1 cells following exposure to NO2. Exp Mol Pathol. 1975; 22:142–150. [PubMed: 163758]
2. Kaplan HP, Robinson FR, Kapanci Y, Weibel ER. Pathogenesis and reversibility of the pulmonary lesions of oxygen toxicity in monkeys. I. Clinical and light microscopic studies. Lab Invest. 1969; 20:94–100. [PubMed: 4988419]
3. Barkauskas CE, et al. Type 2 alveolar cells are stem cells in adult lung. J Clin Invest. 2013; 123:3025–3036. [PubMed: 23921127]
4. Desai TJ, Brownfield DG, Krasnow MA. Alveolar progenitor and stem cells in lung development, renewal and cancer. Nature. 2014; 507:190–194. [PubMed: 24499815]
5. Blanpain C, Fuchs E. Stem cell plasticity. Plasticity of epithelial stem cells in tissue regeneration. Science. 2014; 344:1242281. [PubMed: 24926024]
6. Yanger K, Stanger BZ. Facultative stem cells in liver and pancreas: fact and fancy. Dev Dyn. 2011; 240:521–529. [PubMed: 21312313]

7. Zipori D. The nature of stem cells: state rather than entity. Nat Rev Genet. 2004; 5:873–878. [PubMed: 15520797]
8. Sanchez Alvarado A, Yamanaka S. Rethinking Differentiation: Stem Cells, Regeneration, and Plasticity. Cell. 2014; 157:110–119. [PubMed: 24679530]
9. Borok Z, Danto SI, Lubman RL, Cao Y, Williams MC, Crandall ED. Modulation of t1alpha expression with alveolar epithelial cell phenotype in vitro. Am J Physiol. 1998; 275:L155–164. [PubMed: 9688947]
10. Gonzalez RF, Allen L, Dobbs LG. Rat alveolar type I cells proliferate, express OCT-4, and exhibit phenotypic plasticity in vitro. Am J Physiol Lung Cell Mol Physiol. 2009; 297:L1045–1055. [PubMed: 19717550]
11. Metzger RJ, Klein OD, Martin GR, Krasnow MA. The branching programme of mouse lung development. Nature. 2008; 453:745–750. [PubMed: 18463632]
12. Short K, Hodson M, Smyth I. Spatial mapping and quantification of developmental branching morphogenesis. Development. 2013; 140:471–478. [PubMed: 23193168]
13. Chang DR, et al. Lung epithelial branching program antagonizes alveolar differentiation. Proc Natl Acad Sci U S A. 2013; 110:18042–18051. [PubMed: 24058167]
14. Treutlein B, et al. Reconstructing lineage hierarchies of the distal lung epithelium using single-cell RNA-seq. Nature. 2014; 509:371–375. [PubMed: 24739965]
15. Rawlins EL, Clark CP, Xue Y, Hogan BL. The Id2+ distal tip lung epithelium contains individual multipotent embryonic progenitor cells. Development. 2009; 136:3741–3745. [PubMed: 19855016]
16. Rockich BE, et al. Sox9 plays multiple roles in the lung epithelium during branching morphogenesis. Proc Natl Acad Sci U S A. 2013; 110:E4456–4464. [PubMed: 24191021]
17. Takeda N, et al. Hopx expression defines a subset of multipotent hair follicle stem cells and a progenitor population primed to give rise to K6+ niche cells. Development. 2013; 140:1655–1664. [PubMed: 23487314]
18. Yin Z, et al. Hop functions downstream of Nkx2.1 and GATA6 to mediate HDAC-dependent negative regulation of pulmonary gene expression. Am J Physiol Lung Cell Mol Physiol. 2006; 291:L191–199. [PubMed: 16510470]
19. Takeda N, Jain R, LeBoeuf MR, Wang Q, Lu MM, Epstein JA. Interconversion between intestinal stem cell populations in distinct niches. Science. 2011; 334:1420–1424. [PubMed: 22075725]
20. Herriges M, Morrisey EE. Lung development: orchestrating the generation and regeneration of a complex organ. Development. 2014; 141:502–513. [PubMed: 24449833]
21. Chen F, et al. Hop is an unusual homeobox gene that modulates cardiac development. Cell. 2002; 110:713–723. [PubMed: 12297045]
22. Kim CF, et al. Identification of bronchioalveolar stem cells in normal lung and lung cancer. Cell. 2005; 121:823–835. [PubMed: 15960971]
23. Sakurai MK, Greene AK, Wilson J, Fauza D, Puder M. Pneumonectomy in the mouse: technique and perioperative management. J Invest Surg. 2005; 18:201–205. [PubMed: 16126631]
24. Hogan BL, et al. Repair and regeneration of the respiratory system: complexity, plasticity, and mechanisms of lung stem cell function. Cell Stem Cell. 2014; 15:123–138. [PubMed: 25105578]
25. Alejandre-Alcazar MA, et al. TGF-beta signaling is dynamically regulated during the alveolarization of rodent and human lungs. Dev Dyn. 2008; 237:259–269. [PubMed: 18095342]
26. Cardoso WV, Lu J. Regulation of early lung morphogenesis: questions, facts and controversies. Development. 2006; 133:1611–1624. [PubMed: 16613830]
27. Morrisey EE, Hogan BL. Preparing for the first breath: genetic and cellular mechanisms in lung development. Dev Cell. 2010; 18:8–23. [PubMed: 20152174]
28. Morty RE, Konigshoff M, Eickelberg O. Transforming growth factor-beta signaling across ages: from distorted lung development to chronic obstructive pulmonary disease. Proc Am Thorac Soc. 2009; 6:607–613. [PubMed: 19934357]
29. Dituri F, et al. Differential Inhibition of the TGF-beta Signaling Pathway in HCC Cells Using the Small Molecule Inhibitor LY2157299 and the D10 Monoclonal Antibody against TGF-beta Receptor Type II. PLoS One. 2013; 8:e67109. [PubMed: 23826206]

30. Stange DE, et al. Differentiated Troy+ chief cells act as reserve stem cells to generate all lineages of the stomach epithelium. Cell. 2013; 155:357–368. [PubMed: 24120136]
31. Tata PR, et al. Dedifferentiation of committed epithelial cells into stem cells in vivo. Nature. 2013; 503:218–223. [PubMed: 24196716]
32. Xu X, et al. Evidence for type II cells as cells of origin of K-Ras-induced distal lung adenocarcinoma. Proc Natl Acad Sci U S A. 2012; 109:4910–4915. [PubMed: 22411819]
33. Jackson EL, et al. Analysis of lung tumor initiation and progression using conditional expression of oncogenic K-ras. Genes Dev. 2001; 15:3243–3248. [PubMed: 11751630]
34. Muzumdar MD, Tasic B, Miyamichi K, Li L, Luo L. A global double-fluorescent Cre reporter mouse. Genesis. 2007; 45:593–605. [PubMed: 17868096]
35. Madisen L, et al. A robust and high-throughput Cre reporting and characterization system for the whole mouse brain. Nat Neurosci. 2010; 13:133–140. [PubMed: 20023653]
36. Rock JR, et al. Multiple stromal populations contribute to pulmonary fibrosis without evidence for epithelial to mesenchymal transition. Proc Natl Acad Sci U S A. 2011; 108:E1475–1483. [PubMed: 22123957]
37. Hama H, et al. Scale: a chemical approach for fluorescence imaging and reconstruction of transparent mouse brain. Nat Neurosci. 2011; 14:1481–1488. [PubMed: 21878933]

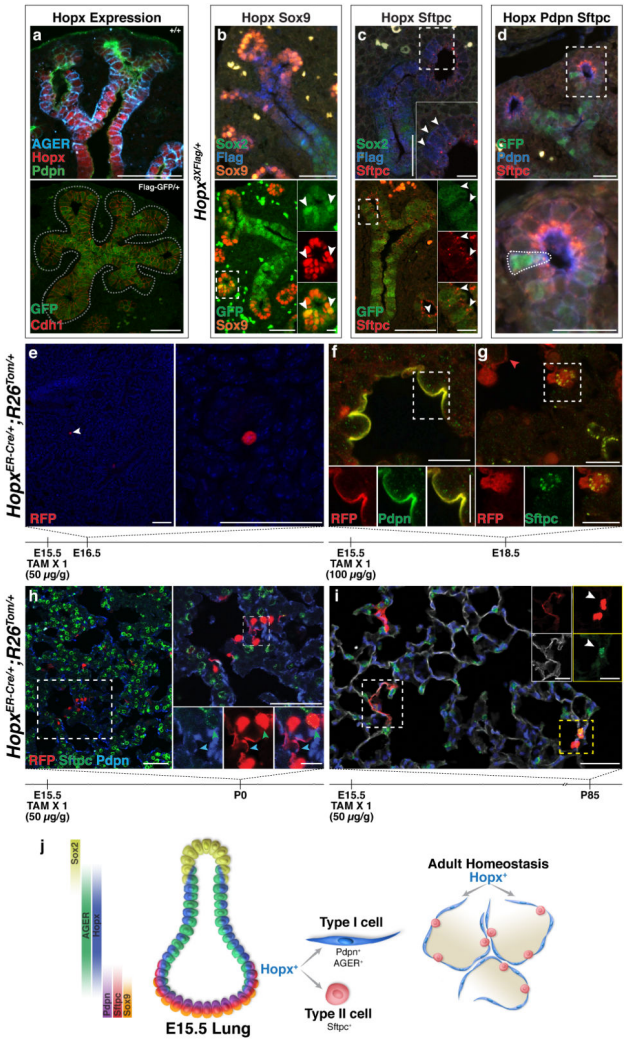

Figure 1. *Hopx* marks bipotent embryonic alveolar progenitors

a-d, Sections of E15.5 lungs showing Hopx expression (*Hopx*$^{3XFlag/+}$ unless otherwise noted). a, Hopx is expressed in distal epithelial cells and the stalk of developing alveolar buds. The top panel is stained with a Hopx antibody. b, A subset of Hopx^{+} cells coexpress Sox9. (Insets show boxed area and arrowheads point to Hopx^{+} Sox9^{+} cells.) c, A subset of Hopx^{+} cells coexpress Sftpc (Insets show high magnification of boxed areas). d, Rare Hopx^{+} cells coexpress Pdpn and Sftpc (bottom panel is high magnification of boxed area in top panel with a triple positive cell outlined). **e-i**, *Hopx*$^{ERCre/+}$*; R26*$^{Tom/+}$ embryos were exposed to one dose of tamoxifen at E15.5 and sacrificed at indicated times. White arrowhead in (e) points to single RFP^{+} cell (magnified image to right). Red arrowhead in (g) points to lineage-labeled Type I cell body and nuclei. Green and blue arrowheads in (h) point to Sftpc^{+} RFP^{+} and Pdpn^{+} RFP^{+} cells, respectively. **j**, Schema of Hopx expression at E15.5 in the developing lung. Scale bars: 10 μm (Insets: b, c, h; f-g), 25 μm (i insets), and 50 μm (a-e, i).

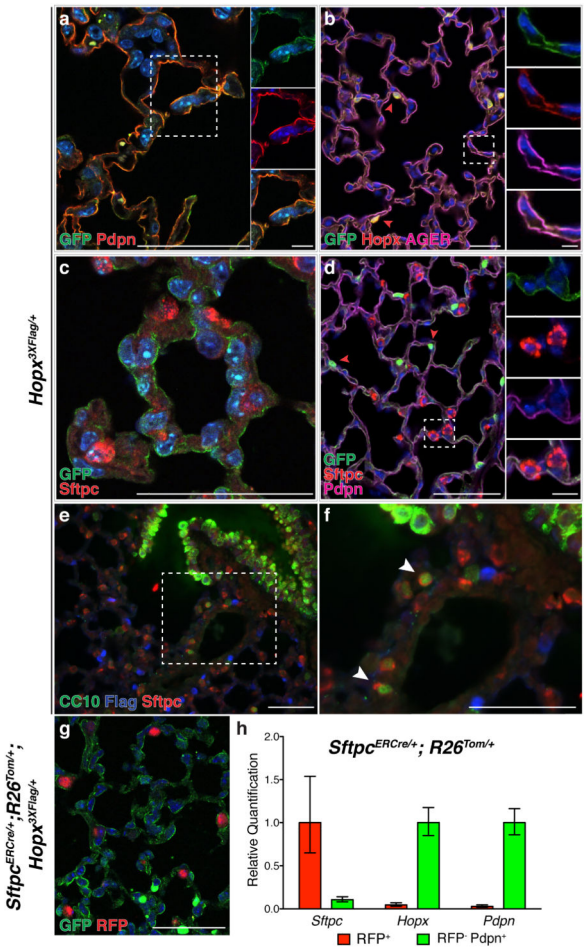

Figure 2. Hopx is restricted to Type I cells in the adult alveolus

a-f, Hopx expression in the adult lung (*Hopx*$^{3XFlag/+}$). Hopx is expressed in Pdpn^{+} cells (a, P133) and AGER^{+} cells (b, P38). Individual channels of boxed areas are shown as insets (a, b; merge is bottom inset in each panel). c-d, Hopx is excluded from Sftpc^{+} cells (c, P90 d, P38). Red arrowheads highlight Hopx^{+}, Type I cell nuclei. (e-f) Sftpc^{+} Scgb1a1^{+} cells (arrowheads in f) do not express Hopx (boxed area in e magnified in f, P133). **g**, *Sftpc*$^{ERCre/+}$*; R26*$^{Tom/+}$*; Hopx*$^{3XFlag/+}$, P167, were dosed with tamoxifen every fifth day for 15 days total (4 doses total) and sacrificed at P186. GFP expression is distinct from Tomato expression. **h**, As assayed by RT-PCR, *Hopx* and *Pdpn* are significantly enriched in the non-lineage labeled, FACS sorted Type I cell population compared to the lineage-labeled, Type II cell population. (Relative quantification (RQ) was normalized to 1 for *Hopx* and *Pdpn* in Type I cell population; RQ 0.046 and 0.029 for *Hopx*, *Pdpn* respectively in Type II cell population.) *Sftpc* expression is significantly lower in the Type I cell population. (RQ normalized to 1 for *Sftpc* in Type II cell population; RQ 0.11 for *Sftpc* in Type I cell population.) Error bars: ± 95% CI. Scale bars: 10 μm (insets a, b, d) and 50 μm (a-g).

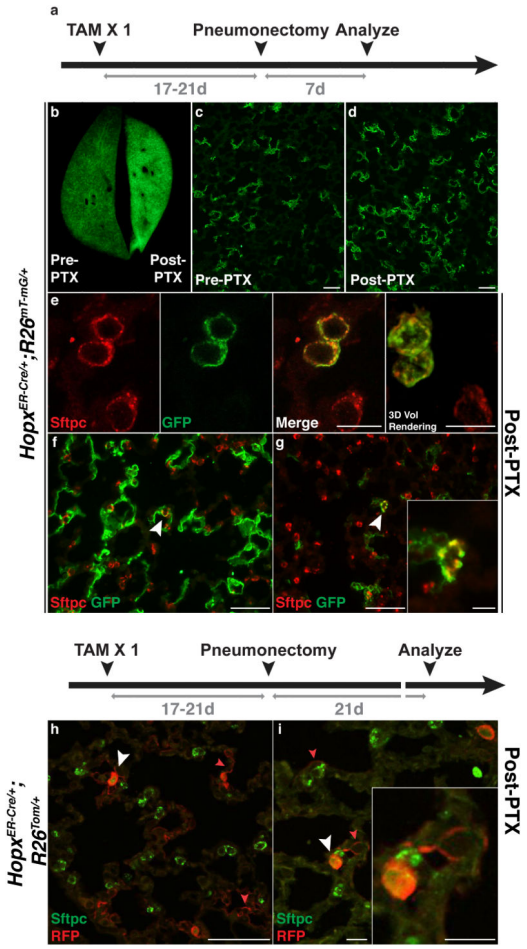

Figure 3. Hopx^{+} cells give rise to Sftpc^{+} cells after pneumonectomy

a, Schema of tamoxifen administration, pneumonectomy, and sacrifice of mice. **b-f**, *Hopx$^{ERCre/+}$; R26$^{mT\text{-}mG/+}$* mice were treated with tamoxifen at P90 and pneumonectomy or sham was performed at P109. Mice were sacrificed 7 days (b-g, n=1 mouse for each pneumonectomy and sham). Whole mount immunofluorescence (b) and GFP expression in lungs pre- and post-pneumonectomy (c and d, respectively). **e-i**, Post-pneumonectomy, Hopx-derived Type I (red arrowhead) and Type II (white arrowhead) cells were identified. Individual channels and merged image of a pair of adjacent Hopx-derived Type II cells is shown in (e), including a 3D volume rendering of a Z-stack through them (e, right panel). (f,g) Two more examples of Hopx-derived Sftpc^{+} cells post-pneumonectomy. (h,i) *Hopx$^{ERCre/+}$; R26$^{Tom/+}$* mice (n=3 each for sham and pneumonectomy) were pulsed with a single dose of tamoxifen (50 mg/kg) at P102, pneumonectomy was performed at P118-121 and mice were sacrificed 21 days later. Insets in g and i shows high magnification of cell highlighted by white arrowhead. Scale bars: 10 μm (e, i; g and i inset), 50 μm (c, d, f-h).

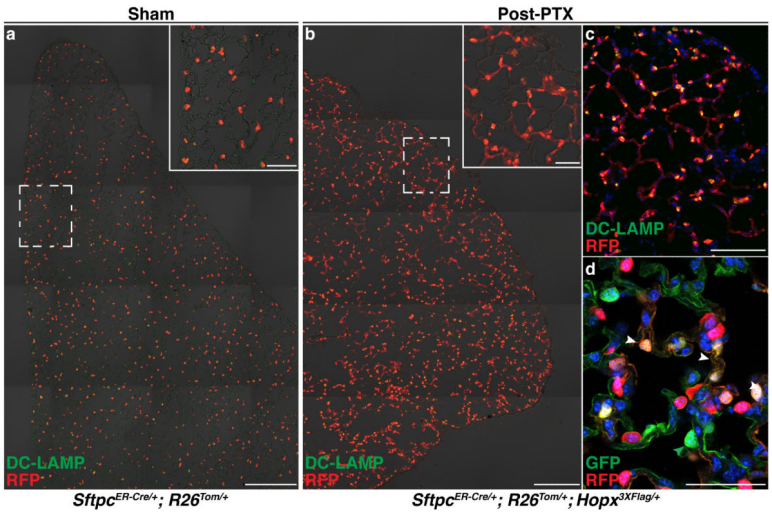

Figure 4. Sftpc^{+} cells give rise to type I cells after pneumonectomy

a-d, Sham (a) or day 21 post-pneumonectomy (b-d) images from *Sftpc$^{ERCre/+}$; R26$^{Tom/+}$* (a) and *Sftpc$^{ERCre/+}$; R26$^{Tom/+}$; Hopx$^{3XFlag/+}$* mice (b-d). White arrowheads in (d) point to lineage labeled, GFP^{+} Type I cells. Green arrowheads in d point to non-lineage labeled Hopx^{+} cells. DC-LAMP is a glycoprotein found in lamellar bodies in mature Type II cells. n=3 mice for each sham and pneumonectomy experiments. Scale bars: 50 μm (a and b insets; d), 100 μm (c), 200 μm (a, b).

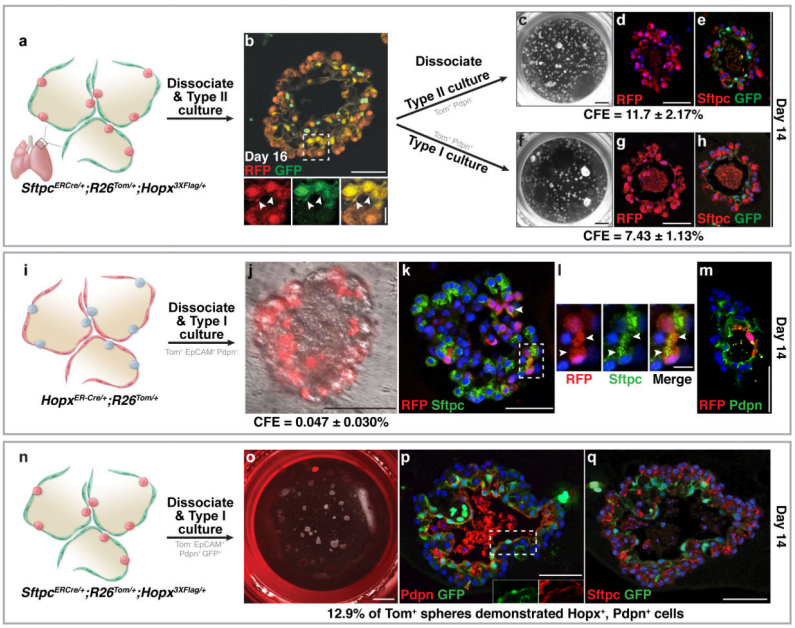

Figure 5. Isolated Hopx^{+}, Type I cells give rise to Type II cells in organoid culture

a, b, Organoids grown from *Sftpc$^{ERCre/+}$; Hopx$^{3XFlag/+}$; R26$^{Tom/+}$* lineage-labeled Type II cells (b) were dissociated and sorted into Type I (Tom^{+} Pdpn^{+}) and Type II (Tom^{+} Pdpn^{-}) cells. Arrowheads in (b, inset) point out RFP^{+} Hopx^{+} cell body. GFP only nuclei represent Pdgfrα+ cells. **c-e**, Type II-derived spheres. **f-h**, Type I-derived organoids were composed of Sftpc^{+} Type II cells and Hopx/GFP^{+} Type I cells. **i-m**, Organoids from Type I cells (EpCAM^{+} Tom^{+} Pdpn^{+}) from *Hopx$^{ERCre/+}$; R26$^{Tom/+}$* lineage labeled alveoli. Rare mosaic spheres containing Tom^{+} cells were observed on day 14. (k-m) Tom^{+} cells co-express Sftpc (k-l, arrowheads). and Pdpn (m). l, High magnification of boxed area in (k). **n-q**, Organoids were generated from Type I cells (Tom^{-} EpCAM^{+} Pdpn^{+} GFP^{+}) from *Sftpc$^{ERCre/+}$; Hopx$^{3XFlag/+}$; R26$^{Tom/+}$* lineage labeled alveoli. (o) Most spheres (mean = 65/well) were Tom^{-} on day 14, and 12.9% of those were Hopx/GFP^{+}. GFP^{-} spheres likely derived from epithelial cells contaminating the stromal population. (p-q) Type I cell-derived organoid composed of Sftpc^{+} Type II cells and Pdpn^{+} Hopx/GFP^{+} Type I cells. Note the cytoplasmic GFP expressed in Pdpn^{+} cells, demonstrating the organoid is not derived from the stromal population (Inset p). Scale bars: 10 μm (b inset; l), 50 μm (b, d, g, k, m, p, q), 100 μm (j), and 1000 μm (c, f, o).

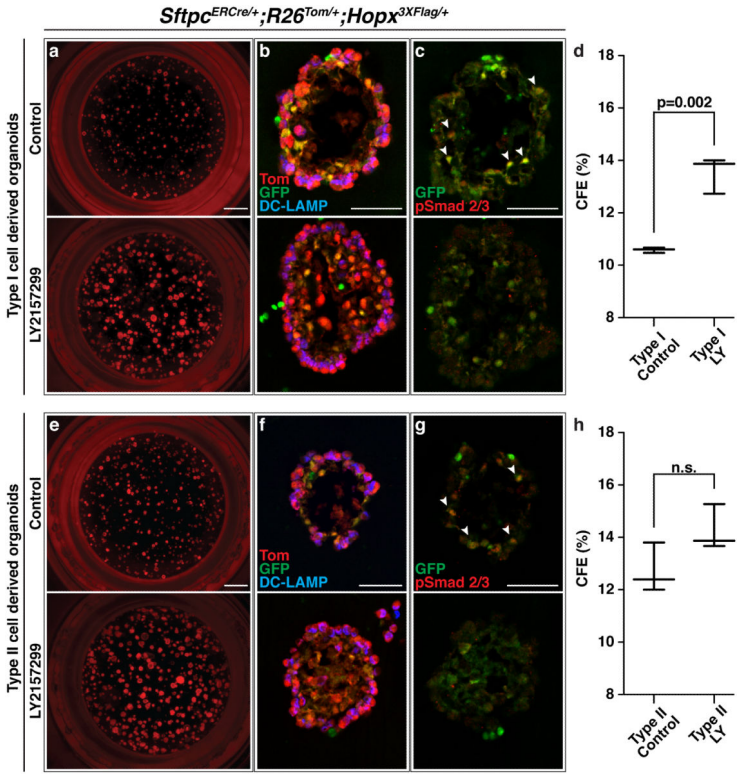

Figure 6. Inhibition of TGFβ increases the rate of conversion of Type I to Type II cells in organoid culture

As in Fig. 4, organoids grown from *Sftpc*$^{ERCre/+}$; *Hopx*$^{3XFlag/+}$; *R26*$^{Tom/+}$ lineage-labeled Type II cells were dissociated and separated into lineage-labeled Type I cells (Tom^{+}Pdpn^{+}GFP^{+}) (a-d) and Type II cells (Tom^{+}Pdpn^{-}GFP^{-}) (e-h). **a-d**, Type I cell derived organoids were grown in the presence of vehicle or the TGFβ inhibitor LY2157299 (LY). (b,c) Day 16 vehicle-treated organoids contain both Type II cells (DC-LAMP^{+}) and Type I cells (HopxGFP^{+}). Many GFP^{+} Type I cells are also pSMAD2/3^{+}, suggesting active TGFβ signaling (white arrowheads). LY-treated organoids also contain both Type II and Type I cells, but they have reduced pSmad 2/3. (d) Day 14 CFE of LY-treated Type I cells is significantly higher than vehicle control (n=3 replicates). **e-h**, Type II cell organoids grown in the presence of LY also contain Type II and Type I cells (f), although there is no difference in the Day 14 CFE between LY-treated organoids and control (h, n=3 replicates). Scale bars: 50 μm (b, c, f, g) and 1000 μm (a, e).

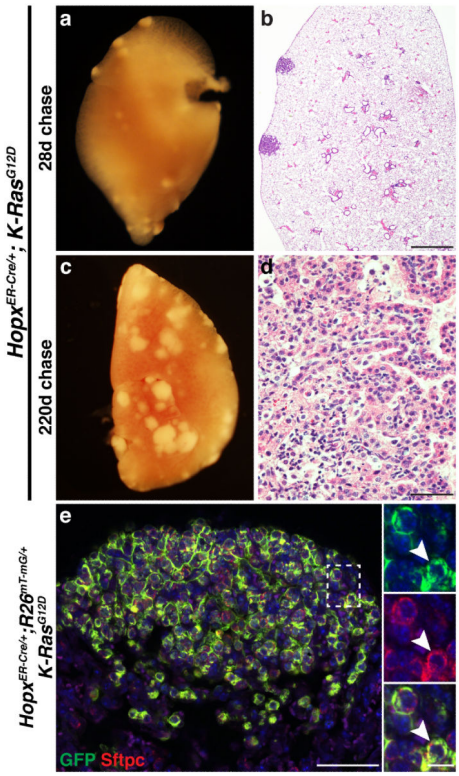

Figure 7. Hopx^{+} cells give rise to tumors in the lung

a-e, *Hopx$^{ERCre/+}$;K-Ras^{G12D}* mice were pulsed with a single dose of tamoxifen between P90 and P100. (a, b) Within 28 days, peripheral tumors formed. (c, d) Longer chases revealed tumors with aggressive features including atypical cells and high mitotic index (d). (e) Hopx-derived tumor cells (GFP^{+}) in *Hopx$^{ERCre/+}$; R26$^{mT-mG/+}$; K-Ras^{G12D}* express Sftpc. Individual channels of highlighted area are shown as insets. Arrowhead indicates a *Hopx*-derived cell that is also Sftpc^{+}. The mouse was pulsed with tamoxifen at P100 and sacrificed 175 days later. Scale Bars: 10 μm (e inset), 50 μm (d, e), and 1000 μm.